Neurobiology of Aging 72 (2018) 62–71

Contents lists available at ScienceDirect

Neurobiology of Aging

journal homepage: www.elsevier.com/locate/neuaging

Paradoxical effects of mutant ubiquitin on Aβ plaque formation in an Alzheimer mouse model

Bert M. Verheijen [a,1], Jo A.A. Stevens [a,1], Romina J.G. Gentier [a,1], Christian D. van 't Hekke [a], Daniel L.A. van den Hove [a,b], Denise J.H.P. Hermes [a], Harry W.M. Steinbusch [a], Jan M. Ruijter [c], Marcus O.W. Grimm [d], Viola J. Haupenthal [d], Wim Annaert [e], Tobias Hartmann [d], Fred W. van Leeuwen [a,*]

[a] Department of Psychiatry and Neuropsychology, Faculty of Health Medicine and Life Sciences, Maastricht University, Maastricht, The Netherlands
[b] Department of Psychiatry, Psychosomatics and Psychotherapy, University of Würzburg, Würzburg, Germany
[c] Department of Medical Biology, Academic Medical Center, Amsterdam, The Netherlands
[d] Deutsches Institut für Demenzprävention, University of Saarland, Experimental Neurology, Homburg, Germany
[e] VIB Center for Brain and Disease Research and KU Leuven, Gasthuisberg, Belgium

ARTICLE INFO

Article history:
Received 11 April 2018
Received in revised form 3 July 2018
Accepted 10 August 2018
Available online 18 August 2018

Keywords:
Mutant ubiquitin
Ubiquitin-proteasome system
γ-Secretase
Amyloid-β
Behavior
Alzheimer's disease

ABSTRACT

Amyloid-β (Aβ) plaques are a prominent pathological hallmark of Alzheimer's disease (AD). They consist of aggregated Aβ peptides, which are generated through sequential proteolytic processing of the transmembrane protein amyloid precursor protein (APP) and several Aβ-associated factors. Efficient clearance of Aβ from the brain is thought to be important to prevent the development and progression of AD. The ubiquitin-proteasome system (UPS) is one of the major pathways for protein breakdown in cells and it has been suggested that impaired UPS-mediated removal of protein aggregates could play an important role in the pathogenesis of AD. To study the effects of an impaired UPS on Aβ pathology in vivo, transgenic APP_{Swe}/PS1ΔE9 mice (APPPS1) were crossed with transgenic mice expressing mutant ubiquitin (UBB^{+1}), a protein-based inhibitor of the UPS. Surprisingly, the APPPS1/UBB^{+1} crossbreed showed a remarkable decrease in Aβ plaque load during aging. Further analysis showed that UBB^{+1} expression transiently restored PS1-NTF expression and γ-secretase activity in APPPS1 mice. Concurrently, UBB^{+1} decreased levels of β-APP-CTF, which is a γ-secretase substrate. Although UBB^{+1} reduced Aβ pathology in APPPS1 mice, it did not improve the behavioral deficits in these animals.

1. Introduction

Alzheimer's disease (AD) is a progressive neurodegenerative disorder and the most common cause of dementia. AD is clinically characterized by progressive memory loss and impairments in multiple cognitive domains (Scheltens et al., 2016). Currently, there is no cure: immunization and γ-secretase inhibitor trials in AD patients have not been effective in terms of reduction of dementia [e.g. (De Strooper, 2014; Hardy and De Strooper, 2017)]. Little is known on the extent to which pathogenic factors drive the development of AD at different stages. To better understand AD, biochemical processes that are thought to underlie the disease should be scrutinized in the context of the cellular phase of AD (De Strooper and Karran, 2016).

One of the neuropathological hallmarks of AD is the presence of extracellular plaques containing aggregated amyloid-β (Aβ) (Goedert and Spillantini, 2006; Gouras et al., 2005; Pensalfini et al., 2014). Aβ peptides are generated via β- and γ-secretase-mediated cleavage of amyloid precursor protein (APP), a type-1 transmembrane glycoprotein of poorly understood function (De Strooper et al., 2010; Müller et al., 2017). Abnormal processing of APP and AD are causally linked, as shown by genetic analysis of (early onset) familial forms of AD and Down syndrome, stressing the importance of this process. According to the "amyloid cascade hypothesis" of AD, Aβ peptides (especially soluble Aβ oligomers), or aggregates thereof in plaques, are the direct cause of the progressive neurodegeneration in AD (Hardy and Selkoe, 2002; Selkoe and Hardy, 2016). Therefore, lowering Aβ levels is a major therapeutic goal in AD. This might be achieved by modulating the production, the aggregation, or the degradation of Aβ.

A growing body of evidence implicates impairment of the ubiquitin-proteasome system (UPS), the main intracellular

* Corresponding author at: Maastricht University, Neuroscience, Maastricht, Netherlands. Tel.: +31 346 56 5146; fax: +31 433 67 1096.
E-mail address: f.vanleeuwen@maastrichtuniversity.nl (F.W. van Leeuwen).
[1] Joint first-authors.

https://doi.org/10.1016/j.neurobiolaging.2018.08.011

proteolytic pathway in eukaryotes, in AD pathogenesis (Ciechanover and Brundin, 2003; Dennissen et al., 2012). A potential role for the UPS in AD is supported by recent genome-wide association studies (GWAS), including pathway analysis and comparative proteomics experiments (International Genomics of Alzheimer's Disease Consortium (IGAP), 2015; Manavalan et al., 2013). In addition, proteasome activity has been shown to be decreased in AD brains (Keller et al., 2001; López Salon et al., 2000).

Interestingly, a frameshift mutant form of ubiquitin (UBB^{+1}) has been found to accumulate in the neuropathological hallmarks of AD patients (Gentier and van Leeuwen, 2015; van Leeuwen et al., 1998). UBB^{+1} is a dose-dependent inhibitor of the UPS (van Tijn et al., 2007), and previous work has demonstrated that UBB^{+1} can induce neurological abnormalities (Fischer et al., 2009; Irmler et al., 2012).

Although there is some evidence for a role of the UPS in APP processing leading to Aβ, and in the clearance of Aβ from cells, the exact contribution of the UPS to Aβ pathology remains poorly understood (Hong et al., 2014; Tseng et al., 2008). A mouse model for Aβ pathology (line 85, carrying familial AD [FAD]-linked APP [$APP_{Swedish}$] and presenilin 1 [PS1ΔE9], hereafter referred to as APPPS1 (Jankowsky et al., 2001, 2004)) was previously crossbred with a mouse line that expresses UBB^{+1} (line 3413) to investigate the effects of long-term UPS inhibition on plaque formation (van Tijn et al., 2012). Unexpectedly, the resulting APPPS1/UBB^{+1} triple transgenic mice showed a decrease in Aβ plaque formation during aging. The mechanisms underlying this phenomenon remain unknown (van Tijn et al., 2012).

In the present study, we show that the paradoxical effect of UBB^{+1} on Aβ load depends on the alteration of γ-secretase activity by UBB^{+1}. γ-secretase activity is reduced in APPPS1 mice, apparently due to PS1ΔE9-induced "poisoning" of the γ-secretase complex (De Strooper, 2007; Woodruff et al., 2013). UBB^{+1} causes a transient increase in PS1-NTF in APPPS1 mice and partially restores γ-secretase activity, lowering the Aβ burden. Although UBB^{+1} reduces Aβ pathology in APPPS1 mice, it does not reduce the behavioral deficits in these animals.

2. Materials and methods

2.1. Animals

Mouse lines were described previously (van Tijn et al., 2012). Line 3413 expresses human UBB^{+1} under control of the murine CamKIIa promoter on a pure C57BL/6 background (Fischer et al., 2009). Distribution of UBB^{+1} is widespread and specific in the brains of these animals (Fischer et al., 2009; Gentier et al., 2015; Verheijen et al., 2017). Transgenic line APPPS1 (line 85, APP_{Swe}/PS1ΔE9), previously described by (Jankowsky et al., 2004), carries a cointegrate of (1) chimeric mouse/human APP695 carrying the Swedish mutation (K594M/N595L) and (2) human PS1 with deletion of exon 9 (Jankowsky et al., 2001), each under control of a mouse prion protein promoter. UBB^{+1}-expressing transgenic mice were crossed with APPPS1 mice to generate APPPS1/UBB^{+1} triple transgenic mice (van Tijn et al., 2012). Transgenic lines were maintained on their respective genetic background by breeding homozygous mice to wild-type (WT) mice for more than 20 generations (Couch et al., 2013). Genotyping was performed by PCR analysis of tail DNA. WT littermates were used as controls. Mice were kept in group housing on a 12/12 hours light-dark cycle with food and water ad libitum in specific pathogen free conditions. Details on animal numbers and tissue collection can be found in the supplementary material. All experimental animal research was executed according to protocols approved by the local Animal Ethical Committee of Maastricht University and met governmental guidelines.

2.2. Immunohistochemistry and image analysis

Immunohistochemistry and image analysis were performed as described previously (van Tijn et al., 2012). In brief, mouse brains were bisected along the midline and sectioned into 50 μm thick sections on a vibratome (Leica VT1000S). To detect and quantify Aβ plaque load, sections were pretreated with formic acid solution (30 minutes) and incubated with mouse monoclonal anti-Aβ antibody 6E10 (1:16,000; Signet 9300-02) overnight. Sections were further processed using the peroxidase-antiperoxidase method and Ni-3,3′-diaminobenzidine color reaction.

For analysis of Aβ plaque load and UBB^{+1} levels, photographs were made using a Zeiss Axioskop microscope with Neofluor 2.5x and 5x objectives and a 558.5 nm bandpass filter (type DMZ-12, ITOS), connected to a Sony XC-77CE CCD black and white camera. Three coronal sections per hemisphere were captured, corresponding to anterior-posterior -1.22, -1.82 and -2.30/2.46 relative to bregma (Paxinos and Franklin, 2001). In each section, the entire cerebral cortex, hippocampus, and dentate gyrus were outlined by hand according to Paxinos et al. (Paxinos and Franklin, 2001) and analyzed. Structure volume (mm^3) and Aβ plaque density (volume percentage) were measured with a custom-made analysis program in Image-Pro Plus software (version 5.1, Media Cybernetics) and Cavalieri's principle of volume estimation (Gundersen and Jensen, 1987). UBB^{+1} levels were determined by measuring the integrated optical density (IOD) of UBB^{+1} staining per outlined brain area. The experimenter was blind to the genotype of the mice.

Aβ plaque density differences between age groups (3, 6, 9, and 11 months) and genotypes (APPPS1 and APPPS1/UBB^{+1}) were compared using two-way analysis of variance (ANOVA) for each of the delineated brain structures (cortex, hippocampus, and gyrus dentatus) using SPSS for Windows (IBM, version 23.0.0.3). Statistical significance was accepted at $p < 0.05$.

2.3. Secretase measurements

Secretase measurements were performed as described previously, with some modifications (Grimm et al., 2013, 2016). Mouse brain tissue (hemispheres) was homogenized using 1.4 mm ceramic beads in a Precellys Minilys (Peqlab, Erlangen, Germany) for 30 seconds at maximum speed in sucrose buffer (10 mM Tris-HCl pH 7.4, 1 mM EDTA, 200 mM sucrose) (without chelator in case of α-secretase measurement). Samples were adjusted to a concentration of 4 mg/mL of total protein using BCA-assay (Smith et al., 1985).

Postnuclear fractions were prepared by centrifuging samples at 900 g for 10 minutes at 4°C. Fractions enriched in membranes were prepared by centrifugation at 55,000 rpm for 75 minutes at 4°C in an Optima MAX Ultracentrifuge with a TLA-55 rotor (Beckman Coulter, Krefeld, Germany). The pellet was solubilized using 0.5 mm glass beads in a Precellys Minilys (Peqlab, Erlangen, Germany) for 10 seconds at minimum speed in sucrose buffer (10 mM Tris-HCl pH 7.4, 1 mM EDTA, 200 mM sucrose). For determination of α-secretase activity, samples were supplemented with 5 μM $ZnCl_2$ and 5 μM $MgCl_2$.

α-, β-, or γ-secretase activities were measured at 37 °C in a black 96-well plate (BD, Franklin Lakes, NJ, USA) by detection of the cleavage of a specific substrate in a Safire2 Fluorometer (Tecan, Germany) for β-secretase activity or in an Infinite M1000 Pro (Tecan, Germany) for α-secretase and γ-secretase activities.

For the determination of γ-secretase activity, 500 μg of protein per 100 μL was used. Kinetics were started by adding 10 μM

γ-secretase substrate (#565764, Calbiochem, Darmstadt, Germany). γ-secretase activity was measured with an excitation wavelength of 355 nm (bandwidth 10 nm) and an emission wavelength of 440 nm (bandwidth 10 nm). Kinetic was carried out for 50 cycles with intervals of 180 seconds.

For α-secretase, the substrate #II-565767 was used, whereas for β-secretase, #IV-565758 was used (both from Calbiochem, Darmstadt, Germany). For measurement of β-secretase activity, samples were diluted 1:1 in PBS, pH 4.5, and 100 μL of this dilution, corresponding to 250 μg of total protein was used. Then, 20 μM of β-secretase substrate IV (Calbiochem, Darmstadt, Germany) was added. β-secretase activity was measured with an excitation wavelength of 345 nm (bandwidth 5 nm) and an emission wavelength of 500 nm (bandwidth 5 nm). Kinetic was carried out for 75 cycles with intervals of 80 seconds.

For determination of α-secretase activity, 100 μL sample, corresponding to 100 μg total protein was measured. The α-secretase substrate II was used (Calbiochem, Darmstadt, Germany) in a final concentration of 3 μM. Measurement parameters were adjusted to an excitation wavelength of 340 nm (bandwidth 10 nm) and an emission wavelength of 490 nm (bandwidth 10 nm). Kinetic was carried out for 70 cycles with intervals of 120 seconds.

Specificity of the assays was monitored by using the following secretase inhibitors: α-secretase: 100 μM GM6001 (Calbiochem, Darmstadt), β-secretase: 2 μM Inhibitor IV (Calbiochem, Darmstadt), and γ-secretase: 20 μM Inhibitor X (Calbiochem, Darmstadt).

Statistical analyses were performed using GraphPad Prism 6 Software (San Diego, CA, USA) by one-way ANOVA, followed by Bonferroni's multiple comparisons test. Values are presented as mean±SEM. Differences between groups were considered significant when $p \leq 0.05$.

2.4. Western blotting

Brain hemispheres were homogenized in lysis buffer consisting of STE buffer (250 mM sucrose, 5 mM Tris-HCl, and 1 mM EGTA, pH 7.4) with 1% Triton X-100 and a mix of protease inhibitors (Roche cOmplete Protease Inhibitor Cocktail, cat. no. 11697498001) and phosphatase inhibitors (2.5 mM sodium pyrophosphate and 1 mM β-glycerol phosphate disodium salt) on ice for 20 minutes. Lysates were centrifuged at 13,000 rpm for 15 minutes at 4°C. Total protein amounts of supernatants were quantified using a standard Bradford assay (Pierce). Absorbance (A: 595 nm; 0.1 s/well) was measured with a Victor^3 plate reader (PerkinElmer) and lysates were diluted in water (Baxter). Samples (final protein concentration: 2 μg/μL) were prepared with sample buffer (4x LDS and 4% 2-mercaptoethanol) and lysis buffer followed by incubation in a heater for 10 minutes at 70°C. From each sample, 20 μg of protein was separated using electrophoresis (40 minutes at 200 V/400 mA) in 1x MES running buffer (Invitrogen) on 4%–12% bis-tris precasted gels (Invitrogen) along with SeeBlue Plus2 marker (Invitrogen). Proteins were blotted (100 V/350 mA overnight at 4°C) onto nitrocellulose membranes (Invitrogen) using 1x transfer buffer (NuPAGE). Membranes were blocked using blocking buffer (5% milk powder, TBS, 0.1% Tween-20) for 1 hour at room temperature (RT).

Primary antibodies (3h at RT) were diluted in blocking buffer (Supplementary Material). Primary antibodies were recognized by horseradish peroxidase-conjugated secondary antibodies (goat anti-mouse (GAMPO) or goat anti-rabbit (GARPO); 1:10,000; 1h at RT). Blots were developed using enhanced chemiluminescence (ECL) Western Blotting kit (PerkinElmer) and measured with a Fuji LAS3000. Protein bands were quantified by measuring pixel intensity using AIDA Image Analyzer v4.27 software (Raytest) and normalized for GAPDH.

Statistical analyses were performed using Mann-Whitney *U*-test. Values are presented as mean±SEM. Differences between groups were considered significant when $p \leq 0.05$.

2.5. Behavior testing

2.5.1. Nest building

Mice were housed for 1 week in single cages containing sawdust. On the day before testing, a piece of cotton (the so-called Nestlet, 5 x 5 cm; Ancare, Bellmore) was introduced in the home cage to permit nesting. The following morning the nests were assessed, according to a five-point scale ranging from 1 to 5: 1 = Nestlet not noticeably touched, 2 = Nestlet partially torn up, 3 = mostly shredded but often with no identifiable nest site, 4 = an identifiable, but flat nest, and 5 = a (near) perfect nest (Deacon, 2006; Deacon et al., 2008).

2.5.2. Spontaneous alternation Y-maze test

Performance in the spontaneous alternation Y-Maze was used to assess spatial working memory. The maze was built out of 3 acrylic arms of 40 cm length arranged at a 120° angle. A mouse was placed in the end of one arm of the Y-maze and was allowed to explore freely during a 6-minute session. The maze was thoroughly cleaned with 70% ethanol between tests. The sequence and total number of arms entered were recorded. The percentage of alternations was calculated as the total number of triads divided by the maximum possible of triads (total number of arm entries minus 2), with a triad defined as a consecutive visit through all 3 arms.

2.5.3. Morris water maze

The Morris water maze (MWM) used was a white circular pool (80 cm in diameter) divided into 4 equal imaginary quadrants for data analysis. The water was made opaque by addition of white nontoxic latex paint; water temperature was maintained at 24±2 °C. A white circular platform (6 cm in diameter) was placed beneath the surface of the water. The swimming patterns of the mice were recorded with a video camera mounted above the center of the pool and analyzed with the EthoVision video-tracking system. The water maze was located in a room with several visual stimuli hanging on the walls to provide spatial cues. The acquisition phase was carried out during 4 to 5 consecutive days. On each training day/session, the mice received 3 consecutive training trials with the hidden platform kept in a fixed position. A different starting location was used for each trial. Mice that were not able to find the platform within 60 seconds were guided to the platform by the experimenter. To assess spatial retention, a 60-second probe trial with the platform removed from the pool was given one day after the last hidden platform trial. The time spent swimming in the quadrants was recorded, and the percentages of time spent in the target quadrant (where the platform was located during hidden platform training) were analyzed.

2.5.4. Contextual and cued fear conditioning

Contextual and cued fear conditioning (FC) was used to assess hippocampal and fear memory. Mice were conditioned in a transparent acrylic chamber (40x40 cm) with a metal grid floor. A sound generator attached to the side of the chamber provided a 70 dB tone (cued conditioned stimulus [CS]) for 20 seconds. Mice were first allowed to explore the chamber for 2 minutes after which 4 trials of paired stimuli were presented, spaced 1 minute apart. During the last 2 seconds of the CS, a foot shock of 0.75 mA was given (unconditioned stimulus [US]). Twenty-four hours after conditioning, contextual freezing behavior was assessed by measuring freezing during 2 minutes in the same cage. One day later, cued recall was tested by placing the mice in a modified chamber (triangular

chamber in which the grid was covered by a textured white floorboard), and freezing was analyzed during the presentation of the tone (4 times). Freezing was analyzed using Etho Vision XT.

2.5.5. Statistics

Comparisons between groups for the behavioral measures were done by a two-way ANOVA, except for the MWM, which was analyzed with repeated measures tests using the different trials as repeated measure. Age and genotype were used as factors. For interaction analysis, one-way ANOVAs on genotype were performed. Fear conditioning data were analyzed with a two-way ANCOVA model, using baseline freezing as a covariate. LSD correction was applied to post hoc analysis. Statistical analysis was performed using SPSS 23 (IBM).

3. Results

3.1. UBB^{+1} reduces Aβ plaque load in APPPS1 mice

Immunohistochemistry was performed on mouse brain slices (WT, UBB^{+1}, APPPS1, and APPPS1/UBB^{+1}) and Aβ plaque load in the cerebral cortex and hippocampus was quantified. This analysis revealed an unexpected age-dependent decrease of Aβ plaque load in the AD model expressing UBB^{+1} (Fig. 1). For each of the brain structures, two-way ANOVA showed significant effects of age and genotype on Aβ plaque density, but no significant interaction between age and genotype for APPPS1 and APPPS1/UBB^{+1}. The absence of a significant interaction effect indicates that the genotype effect is independent of the age group and thus that the phenotype effect is present at every age. The same test was performed on Aβ plaque density for the genotypes WT and UBB^{+1}. This test showed no significant effects of age or genotype. These findings corroborate previous findings on a modulating effect of UBB^{+1} on Aβ pathology in mice (van Tijn et al., 2012), showing a decrease in plaque load over a prolonged period of time. No changes in Aβ plaque microenvironment were observed (i.e., reactive gliosis [(van Tijn et al., 2012) and not shown]). Aβ accumulation did not induce additional accumulation of UBB^{+1} (van Tijn et al., 2012).

3.2. UBB^{+1} partially restores γ-secretase activity in APPPS1 mice

To evaluate the effects of AD mutations and UBB^{+1} on flux through the amyloidogenic pathway, measurements of α-, β-, and γ-secretase activities were carried out on mouse brain tissue. Hemispheres from different mouse lines (WT, UBB^{+1}, APPPS1, and APPPS1/UBB^{+1}) of different ages (3M, 6M, and 9M) were lysed and subjected to enzymatic assays (Fig. 2). α- and β-secretase activities were unaltered in all mouse lines. γ-secretase was significantly and specifically decreased in APPPS1 mice at all ages. In APPPS1 mice, a slight increase in γ-secretase activity was observed at 9M, as compared to APPPS1 mice at earlier ages. However, these differences were not statistically significant (6M vs. 9M: $p = 0.15$). In the APPPS1/UBB^{+1} line, a partial but significant restoration of γ-secretase activity was observed at 6M. γ-secretase activity in APPPS1/UBB^{+1} mice was comparable at all ages tested. These results show

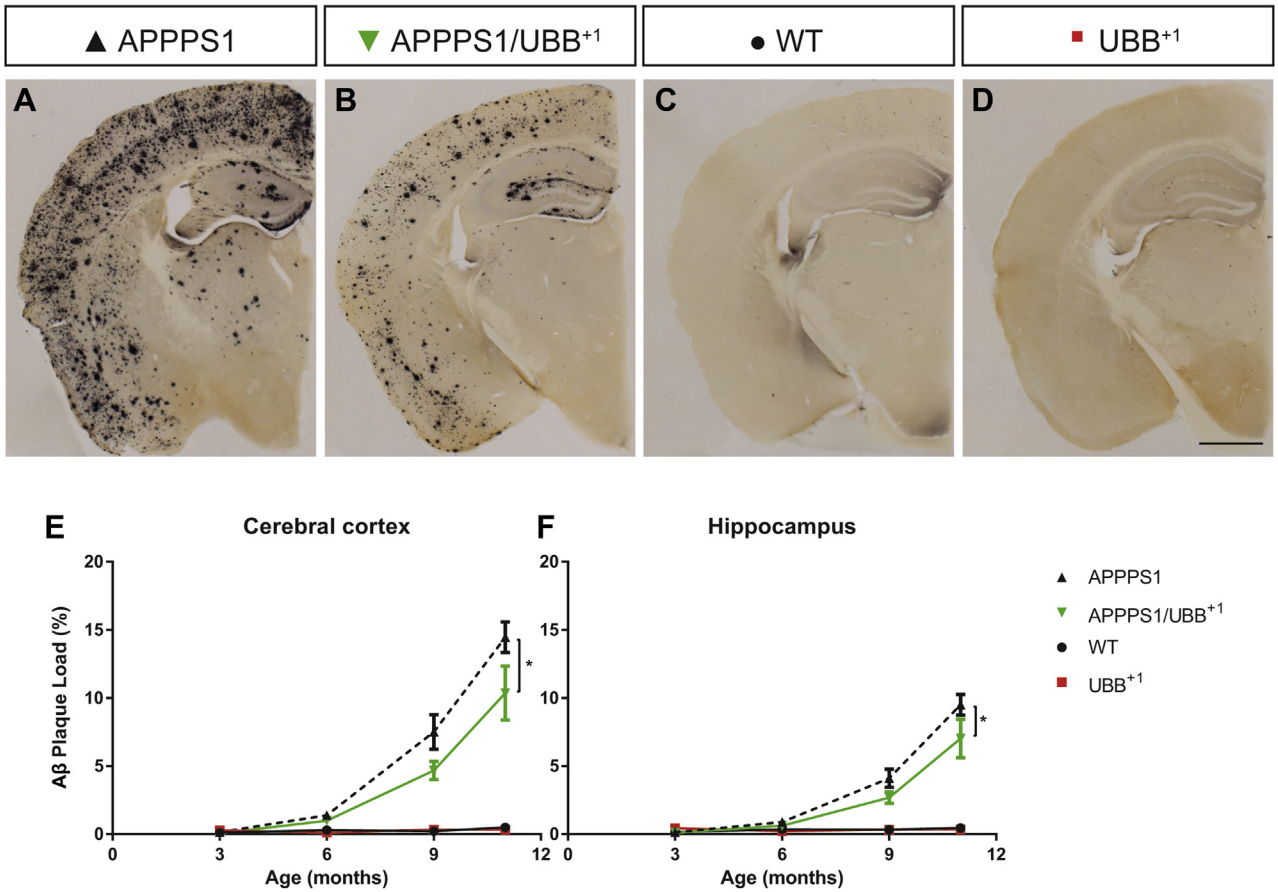

Fig. 1. UBB^{+1} decreases Aβ plaque load in APPPS1 mice. Quantitative immunohistochemical representation by integrated optical densities of Aβ plaque load (E, F) in 4 different mouse lines (A–D). A clear decrease in Aβ plaque load could be observed in the APPPS1/UBB^{+1} line (vs. APPPS1 mice). Values are presented as mean ± SD. $^{*}p \leq 0.05$. Bar: 1 mm.

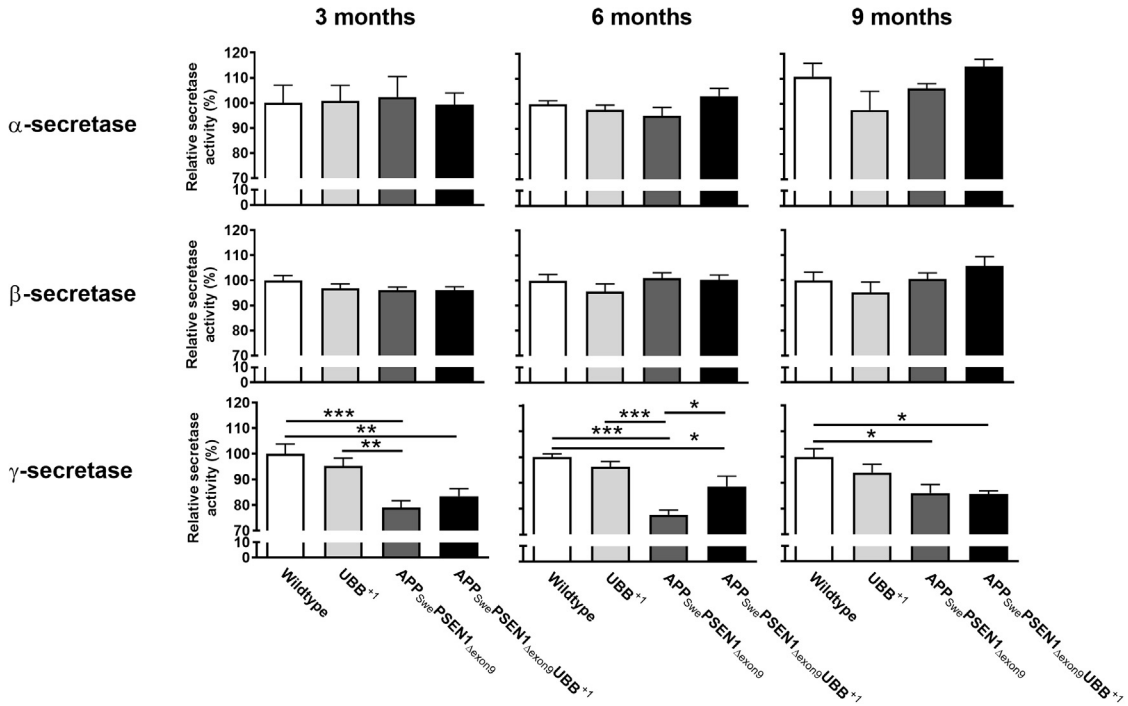

Fig. 2. UBB^{+1} partially restores γ-secretase activity in APPPS1 mice. Secretase activity measurements in 4 mouse lines reveal that α- and β-secretase activities do not significantly differ between mice. In the APPPS1 and APPPS1/UBB^{+1} triple tg mice, γ-secretase activity was significantly decreased at 3, 6, and 9 months of age as compared to WT and UBB^{+1} mice. However, in APPPS1/UBB^{+1} mice, the γ-secretase activity was partially restored at the age of 6 months (vs. APPPS1 mice). $^{*}p \leq 0.05$; $^{**}p \leq 0.01$; $^{***}p \leq 0.001$.

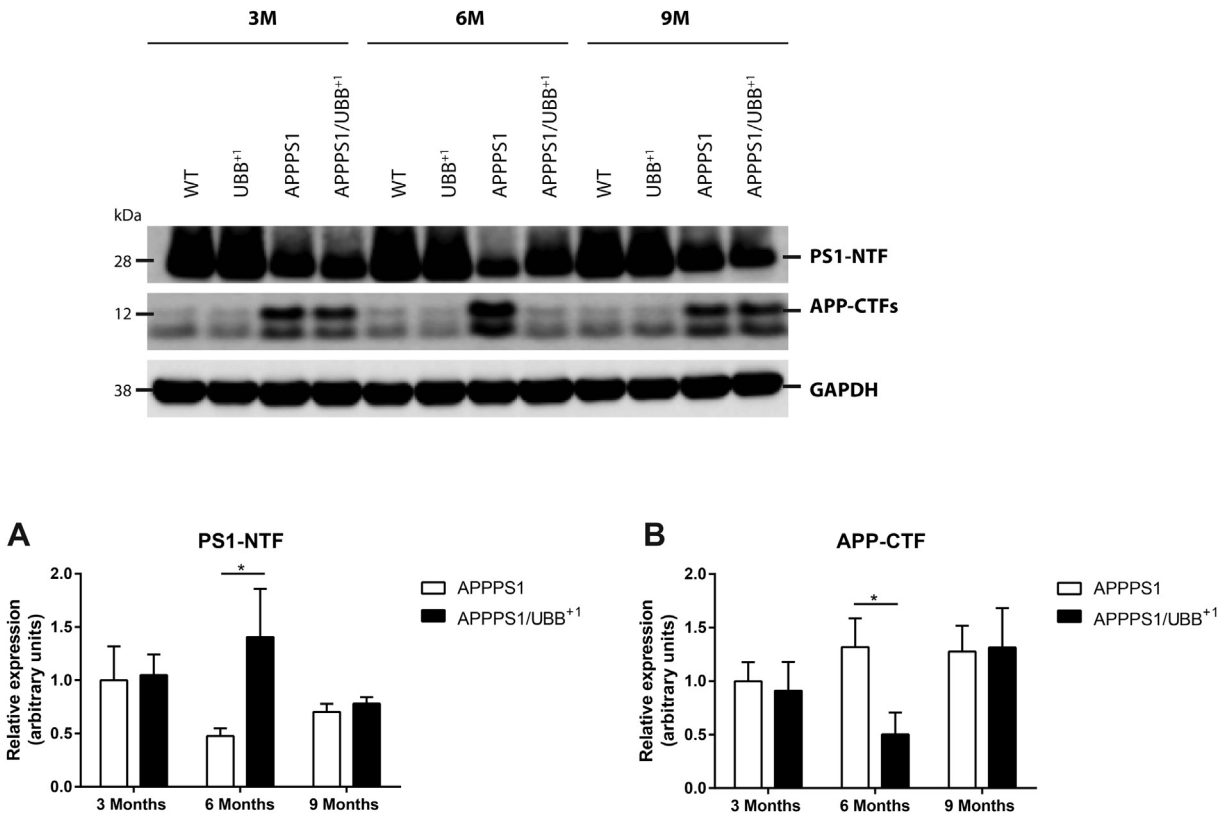

Fig. 3. UBB^{+1} temporarily increases PS1-NTF levels and lowers levels of APP-CTF in APPPS1 mice. Protein expression levels of the PS1-NTF and β-APP-CTF were measured in immunoblotting experiments. APP-CTF expression was normalized against APP-FL expression and all expression values were normalized against GAPDH. Significantly increased ($^{*}p \leq 0.01$) PS1-NTF levels (A) and significantly decreased ($^{*}p \leq 0.01$) APP-CTF levels (B) were found to be present in APPPS1/UBB^{+1} mice as compared to APPPS1 mice at 6 months of age. Representative blots are shown.

that γ-secretase activity is decreased in APPPS1 mice and that UBB^{+1} partially rescues this activity at 6M.

3.3. UBB^{+1} transiently increases PS1-NTF levels and reduces APP-CTFs in APPPS1 mice

Immunoblots for different components of the γ-secretase complex were performed to explore a link between UBB^{+1} expression and partial increase in γ-secretase activity. Only PS1-NTF, the processed form of PS1 that is present as a PS1-NTF-CTF heterodimer complex (Edbauer et al., 2003; Thinakaran et al., 1996), was found to be significantly increased in APPPS1/UBB^{+1} mice at 6M (Fig. 3). In addition, APP-CTF (C99) was significantly down-regulated in APPPS1/UBB^{+1} mice, consistent with increased γ-secretase activity (Fig. 3). A complete overview of immunoblotting experiments can be found in the Supplementary Material.

3.4. UBB^{+1} does not improve behavioral outcome in APPPS1 mice

Mice were subjected to a variety of behavioral tests to assess memory and other behavioral parameters in the 4 strains at different ages (Fig. 4). Differences in performance might indicate a modifying effect of Aβ load on functional outcomes.

First, nest building behavior was assessed (Fig. 4A and B). Nest building activity is a spontaneous behavior and represents mouse wellbeing. APPPS1 and APPPS1/UBB^{+1} triple transgenic mice showed significantly impaired nest building behavior in comparison with WT and UBB^{+1} mice ($p < 0.05$ in all cases, Fig. 4B). There were no differences in nest building activities between WT and UBB^{+1} mice or between APPPS1 and APPPS1/UBB^{+1} mice. Differences in nest building activity remained present as animals aged.

Next, working memory was assessed in the alternating Y-maze. No significant differences were present in any of the strains in the percentage of alternations (Fig. 4C). A trend showing more entries for APPPS1 and APPPS1/UBB^{+1} mice as compared to WT controls was observed (data not shown).

In addition, the MWM test was used as a test of spatial memory performance. Although there was no difference in acquisition time between the strains, APPPS1 and APPPS1/UBB^{+1} mice spent significantly less time in the target quadrant during the probe trial in comparison to WT animals ($p < 0.05$), but not compared to UBB^{+1} animals. There was no difference between ages (Fig. 4D and E).

The contextual FC is mostly hippocampus-dependent, whereas the cued FC test mainly indicates integrity of the amygdala and cerebellum (Buccafusco, 2009). The contextual FC tests showed no impairment of memory between any of the strains at any of the tested ages (Fig. 4F). However, all 9-month-old animals performed significantly worse than young animals ($p < 0.001$). UBB^{+1} mice had impaired cued FC memory compared to WT and APPPS1 mice ($p < 0.01$) but performed similarly to APPPS1/UBB^{+1} mice at 3 months of age (Fig. 4G). At 6 months of age, UBB^{+1}, APPPS1, and APPPS1/UBB^{+1} mice all performed worse than WT mice ($p < 0.001$). APPPS1 mice had the most severe memory problems, scoring significantly lower than UBB^{+1} mice ($p < 0.001$), but interestingly APPPS1/UBB^{+1} performed better than APPPS1 mice ($p < 0.05$), matching the altered Aβ load. At 9 months of age, no significant differences between groups could be detected, although there was a trend for APPPS1/UBB^{+1} mice to perform worse than WT mice ($p = 0.054$). This lack of difference could be due to the poor performance of the older mice in general, with 9-month-old mice scoring significantly lower than young mice ($p < 0.001$).

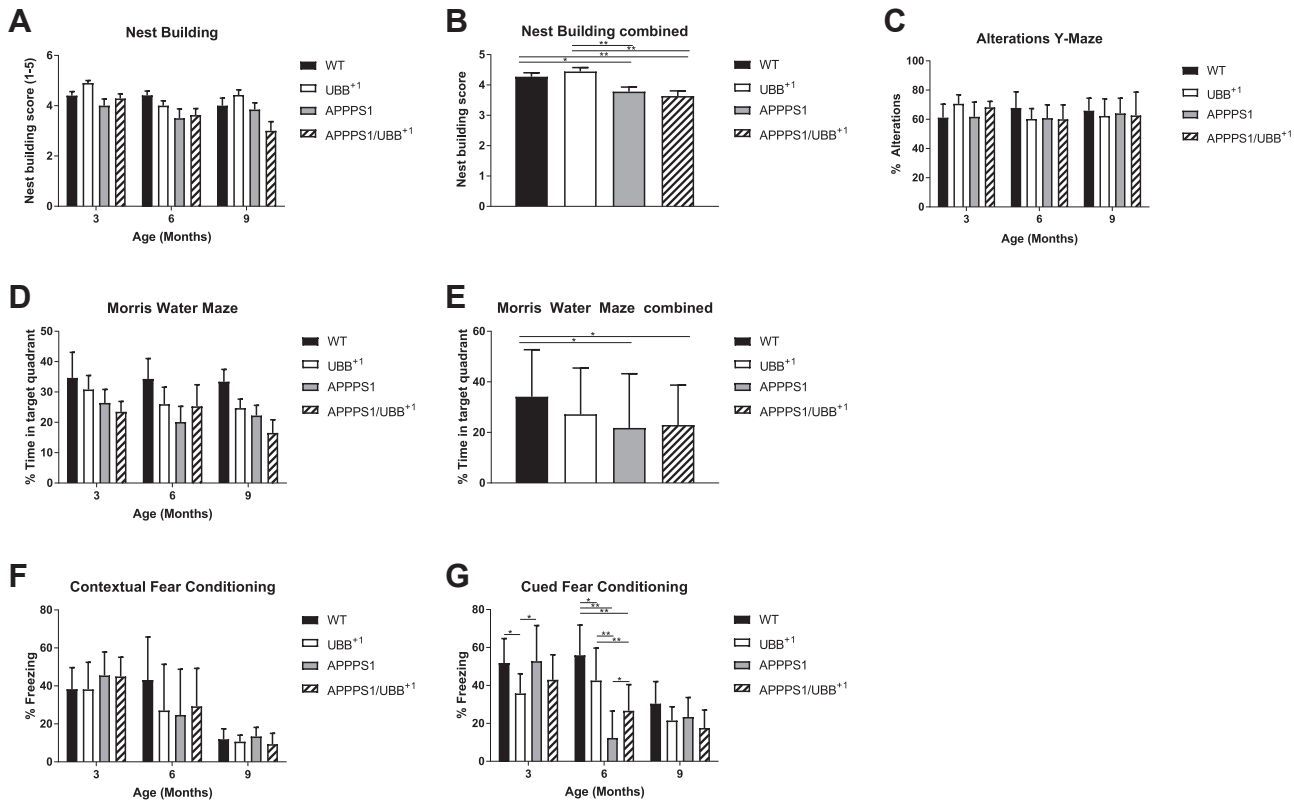

Fig. 4. UBB^{+1} does not improve behavioral phenotypes in APPPS1 mice. Mouse strains of different ages were tested using several behavioral assays, including nest building (A, B), Y-maze (C), Morris Water Maze (D, E), and fear conditioning paradigms (F, G). Values are presented as mean ± SD (SEM in E). Combined groups (B, E) include animals of different genotypes, regardless of age. *$p \leq 0.05$; **$p \leq 0.01$. No overall improvements in behavioral phenotypes were observed in APPPS1/UBB^{+1} mice (vs. APPPS1 mice).

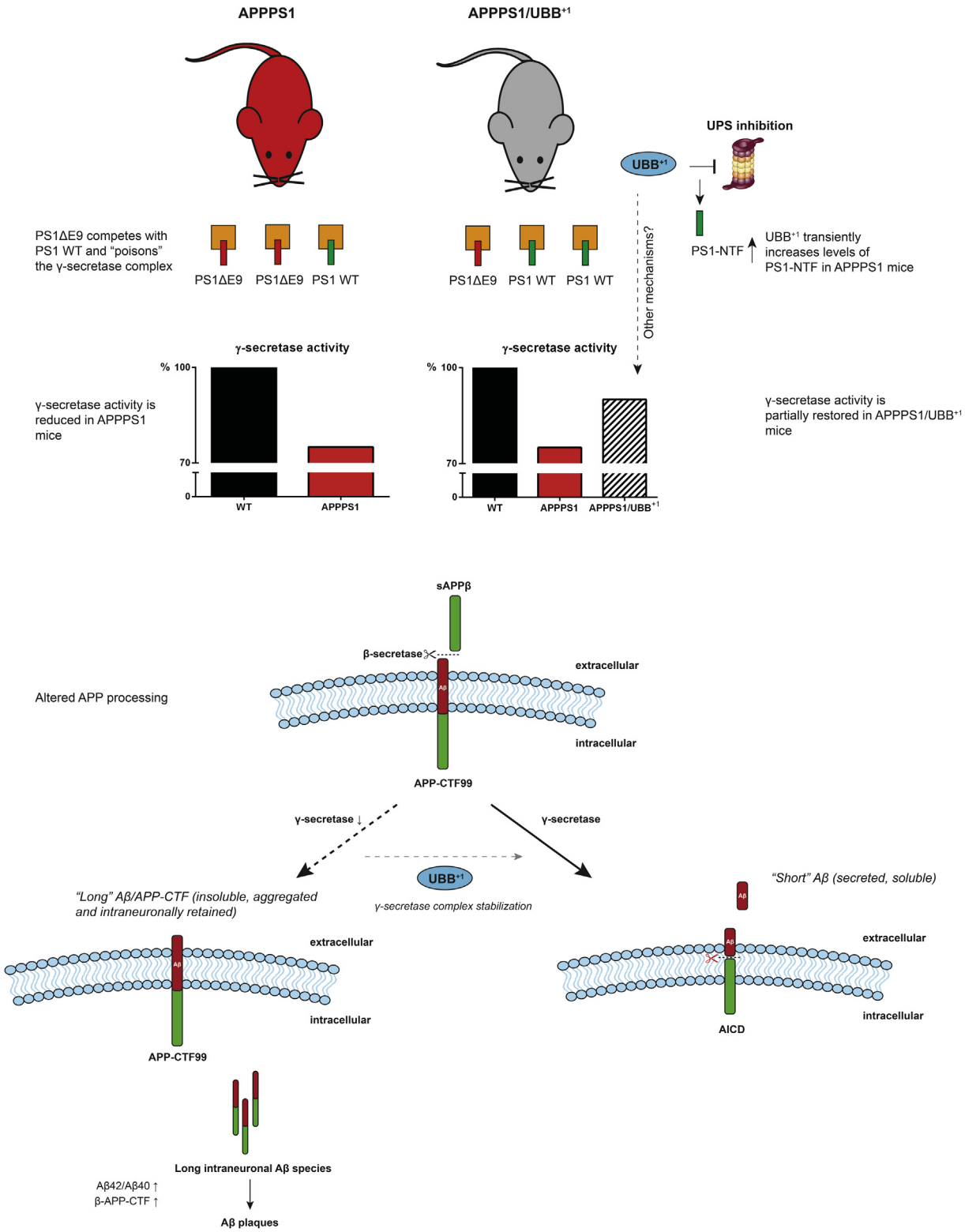

Fig. 5. Effects of UBB^{+1} on APP processing in APPPS1 mice. Schematic illustration of changes in APPPS1 mice and in APPPS1 mice coexpressing UBB^{+1}. In APPPS1 mice, PS1dE9 competes with wild-type PS1, antagonizing γ-secretase activity. Reduced γ-secretase activity results in less efficient processing of β-secretase-derived C99 fragments (β-APP-CTFs) in the amyloidogenic pathway, resulting in intraneuronally retained long hydrophobic APP metabolites and formation of plaques. UBB^{+1} induces a transient increase of PS1-NTF in APPPS1 mice, resulting in partial restoration of γ-secretase activity and increased processing of APP.

4. Discussion

UBB^{+1} was found to decrease Aβ burden in APPPS1 mice (van Tijn et al., 2012), a mouse line in which the development and progression of Aβ pathology have been described in detail (Garcia-Alloza et al., 2006; Janus et al., 2015; Volianskis et al., 2010). In the present study, we showed that this UBB^{+1}-mediated effect depends, at least in part, on partial restoration of γ-secretase activity

in APPPS1 mice (Fig. 5). Preserved γ-secretase activity resulted in reduced levels of β-APP-CTF and decreased Aβ42 levels (van Tijn et al., 2012).

Specifically, γ-secretase activity in APPPS1/UBB^{+1} mice was temporarily increased compared to APPPS1 mice at 6 months of age, a critical period of plaque formation (Tucker et al., 2008). Understanding the precise mechanisms underlying these UBB^{+1}-induced changes will be important to explain the rather unexpected effect of UBB^{+1} on Aβ pathology.

Immunoblotting revealed that PS1-NTF levels were also increased in triple transgenic mice at the 6M timepoint. PS1ΔE9 that is present in APPPS1 mice cannot be endoproteolytically processed by "presenilinase" activity. Presenilinase has been described as an unknown protease that is required for the normal function of PS1 in the γ-secretase complex (Podlisny et al., 1997), but it has become clear that autoproteolysis probably cleaves PS1 (Fukumori et al., 2010; Wolfe et al., 1999). Therefore, UBB^{+1} increased levels of WT PS1-NTF in APPPS1 mice. UBB^{+1} might regulate PS1-NTF protein expression through several mechanisms: i) UBB^{+1} may increase WT PS1 protein expression because WT PS1 holoprotein has been previously shown to be degraded by the UPS (Fraser et al., 1998). However, levels of full-length PS1 were found to be unaltered in APPPS1/UBB^{+1} mice in preliminary experiments (Supplementary Material); ii) UBB^{+1} might regulate PS1 processing (i.e., affect presenilinase activity), and iii) UBB^{+1} may regulate stability of PS1-NTF(/CTF) fragments (Steiner et al., 1998). We cannot exclude a role for other factors in regulating PS1-NTF levels and γ-secretase activity that are affected by UBB^{+1}. In APPPS1 mice, an age-related trend toward increased γ-secretase activity was observed, although this was not statistically significant. Perhaps sustained γ-secretase inhibition results in a subtle compensatory rebound, for example, by altering PS1 turnover.

To fully appreciate the complexity of the effects of UBB^{+1} on APP metabolism and Aβ pathology, it should be noted that UBB^{+1}-mediated effects might be due to interference with other pathways, independent of proteasome inhibition. For example, UBB^{+1} can signal via K63-linkage (e.g., regulating neuroinflammation) (Ohtake et al., 2016; van Tijn et al., 2012) acts as an inhibitor of specific deubiquitinating enzymes (DUBs) (Krutauz et al., 2014), affects mitochondrial functioning (Braun et al., 2015; Tan et al., 2007), and potentially impacts neuronal activity and synaptic function/long-term synaptic potentiation.

We propose that a combination of UBB^{+1}-dependent changes is most likely to explain the ameliorating effect of UBB^{+1} on Aβ load in vivo. Perhaps most interestingly, UBB^{+1} induces chaperone expression (heat shock proteins, 14-3-3ζ) in cells, potentially conferring cytoprotective effects (Hope et al., 2003; Irmler et al., 2012). Modulation of protein quality control mechanisms beyond the proteasome would provide an attractive model to explain diminished Aβ load in an environment of chronic UBB^{+1} expression. This is supported by studies pointing out a role for intracellular trafficking and the endosomal-lysosomal pathway in APP processing, as well as in Aβ degradation, secretion, and propagation (Almeida et al., 2006; Nixon, 2017; Otero et al., 2018; Small et al., 2017). Specificity of intramembrane proteolysis probably depends on differential localization of distinct γ-secretase complexes and substrates at the cell surface and at endosomes (Sannerud et al., 2016). The respective roles of different APP degradation pathways are poorly understood. With respect to APP-CTF degradation, we suggest that, under physiological conditions, β-APP-CTFs are mostly cleaved by γ-secretase to produce shorter Aβ peptides. Remaining APP-CTFs are cleared via the endolysosomal pathway or by alternate proteasome-dependent pathways, like endoplasmic reticulum-associated degradation. By interfering with secretase processivity in AD, the role of these nonsecretase-dependent degradation pathways changes because more intraneuronal APP-CTFs need to be turned over via these mechanisms. UBB^{+1} could play a crucial role in this rerouting and in the cross-talk between different protein degradation systems.

In summary, the mechanism we propose for the paradoxical decrease in Aβ burden by UBB^{+1} expression in mouse brain is manifold and depends on: i) a partial rescue of γ-secretase activity and APP processing, through transiently restoring PS1 levels, presumably by regulating (UPS-mediated) PS1 turnover (this study), ii) induction of molecular chaperones, which decrease Aβ aggregation and improve the clearance of Aβ from brains, and iii) changes in intracellular transport, localization, and the endolysosomal pathway (to be investigated).

Notably, UBB^{+1} did not improve the overall behavioral phenotype in APPPS1 mice. This may be due to several factors. First, the decrease in Aβ burden in APPPS1/UBB^{+1} mice is relatively mild. After the onset of Aβ pathology, irreversible damage may have already occurred, for example, through persistent neuroinflammation. Also, pre-existing Aβ burden appeared hard to remove in mice (Tucker et al., 2008). There might be a role for residual Aβ oligomers affecting the behavior. In addition, UBB^{+1} can induce behavioral defects itself (Fischer et al., 2009; Irmler et al., 2012), which could counteract the beneficial effect of reducing the Aβ load. In addition, γ-secretase has many other substrates besides APP and interfering with its activity could affect other processes at an early stage (De Strooper et al., 2012; Jurisch-Yaksi et al., 2013; Kopan and Ilagan, 2004). Lack of statistical power may also explain the absence of improved behavioral phenotypes. Initially, more mice were included in the experimental groups, but several mice had to be excluded due to the occurrence of seizures in these animals (confirmed by neuropeptide Y immunostainings, unpublished). Aβ is known to elicit epileptiform activity (Minkeviciene et al., 2009; Palop and Mucke, 2010). More detailed behavioral analyses, including larger group sizes, will provide better insights into these phenotypes.

The present findings may have important translational implications. It has previously been suggested to use γ-secretase activity inhibition as a therapeutic approach in AD. However, some studies have indicated that maintaining healthy γ-secretase activity, rather than inhibiting it, should be considered as a therapeutic strategy in AD (Barnwell et al., 2014; Woodruff et al., 2013). Inhibiting γ-secretase activity in patients has actually been associated with adverse events, such as skin cancers and infections (Doody et al., 2013). Our present data add another level of complexity to targeting γ-secretase function in AD.

Importantly, most presenilin FAD mutations give rise to overall lower Aβ levels, but rather shift the Aβ profile (so, a quantitative [lower] as well as qualitative [longer Aβ] effect). Silencing expression of mutant alleles and pathological factors, for example, using antisense therapies or by targeting protein-protein interactions, could prove beneficial to patients. Modulators and stabilizers of γ-secretase that lower Aβ without inhibiting general γ-secretase activity, for example, by restoring the carboxypeptidase-like trimming function disrupted by mutant PS1, are also of considerable interest (Chávez-Gutiérrez et al., 2012; Szaruga et al., 2017; Voytyuk et al., 2018). Future studies should explore the pathogenic mechanisms that drive AD in more detail: by restrictively modifying the expression of AD-associated factors, for example, those implied in the amyloidogenic pathway and the UPS, one should be able to accurately pinpoint key targets that modify disease phenotypes. These studies should also incorporate other aspects of AD pathology, like tau pathology and synaptic function, and should address the contribution of additional processes and cell types (De Strooper and Karran, 2016; Hong et al., 2016; Lin et al., 2018; Sosna et al., 2018; Venegas et al., 2017). Ultimately, it will be possible to

establish in vivo dose-response curves and determine critical periods in AD pathology (e.g., using other UBB^{+1}-expressing transgenic mouse lines (van Tijn et al., 2010)), providing crucial insights for therapeutic approaches.

5. Conclusion

UBB^{+1} decreases Aβ plaque load in APPPS1 mice through modulating γ-secretase activity and reducing production of long Aβ species (i.e., APP-CTFs, long Aβ oligomers) (Fig. 5). Preserving physiological γ-secretase activity at an early stage, rather than inhibiting it, should be explored as a therapeutic option in AD. The effects of UBB^{+1} on cells are more complex than previously appreciated and should be investigated in more detail in future studies.

Disclosure statement

The authors report no conflicts of interest.

Acknowledgments

FWvL was supported by ISAO (#06502 and 09514) and Hersenstichting Nederland (2008.17 and 15F07.48). Prof. D.A. Hopkins (Dalhousie University, Halifax, NS, Canada) is acknowledged for critical evaluation of an early version of the article and was supported by an ISAO Visiting Professorship and by the Department of Neuroscience of Maastricht University. We thank V. Baert for help with the immunoblotting experiments. J.J. Cheng is acknowledged for performing behavioral assays. We are grateful to Prof. D.R. Borchelt (Center for Translational Research in Neurodegenerative Disease, Department of Neuroscience, Gainesville, FL, USA) for providing the original APP$_{Swe}$/PS1ΔE9 mouse line (line 85). WA is supported by VIB, KU Leuven (C16/15/073), the federal government (IAP P7/16), the FWO (S006617N, G078117N and G056017N) and SAO (S#16018).

Appendix A. Supplementary data

Supplementary data related to this article can be found at https://doi.org/10.1016/j.neurobiolaging.2018.08.011.

References

Almeida, C.G., Takahashi, R.H., Gouras, G.K., 2006. Beta-amyloid accumulation impairs multivesicular body sorting by inhibiting the ubiquitin-proteasome system. J. Neurosci. 26, 4277–4288.

Barnwell, E., Padmaraju, V., Baranello, R., Pacheco-Quinto, J., Crosson, C., Ablonczy, Z., Eckman, E., Eckman, C.B., Ramakrishnan, V., Greig, N.H., Pappolla, M.A., Sambamurti, K., 2014. Evidence of a novel mechanism for partial γ-secretase inhibition induced paradoxical increase in secreted amyloid β protein. PLoS One 9, e91531.

Braun, R.J., Sommer, C., Leibiger, C., Gentier, R.J.G., Dumit, V.I., Paduch, K., Eisenberg, T., Habernig, L., Trausinger, G., Magnes, C., Pieber, T., Sinner, F., Dengjel, J., van Leeuwen, F.W., Kroemer, G., Madeo, F., 2015. Accumulation of basic amino acids at mitochondria dictates the cytotoxicity of aberrant ubiquitin. Cell Rep 10, 1557–1571.

Buccafusco, J.J., 2009. Methods of behavior analysis in neuroscience, second ed. CRC Press/Taylor & Francis.

Chávez-Gutiérrez, L., Bammens, L., Benilova, I., Vandersteen, A., Benurwar, M., Borgers, M., Lismont, S., Zhou, L., Van Cleynenbreugel, S., Esselmann, H., Wiltfang, J., Serneels, L., Karran, E., Gijsen, H., Schymkowitz, J., Rousseau, F., Broersen, K., De Strooper, B., 2012. The mechanism of γ-Secretase dysfunction in familial Alzheimer disease. EMBO J. 31, 2261–2274.

Ciechanover, A., Brundin, P., 2003. The ubiquitin proteasome system in neurodegenerative diseases: sometimes the chicken, sometimes the egg. Neuron 40, 427–446.

Couch, B.A., Kerrisk, M.E., Kaufman, A.C., Nygaard, H.B., Strittmatter, S.M., Koleske, A.J., 2013. Delayed amyloid plaque deposition and behavioral deficits in outcrossed AβPP/PS1 mice. J. Comp. Neurol. 521, 1395–1408.

De Strooper, B., 2014. Lessons from a failed γ-secretase Alzheimer trial. Cell 159, 721–726.

De Strooper, B., 2007. Loss-of-function presenilin mutations in Alzheimer disease. Talking Point on the role of presenilin mutations in Alzheimer disease. EMBO Rep. 8, 141–146.

De Strooper, B., Iwatsubo, T., Wolfe, M.S., 2012. Presenilins and γ-secretase: structure, function, and role in Alzheimer Disease. Cold Spring Harb Perspect. Med. 2 a006304–a006304.

De Strooper, B., Karran, E., 2016. The cellular phase of Alzheimer's disease. Cell 164, 603–615.

De Strooper, B., Vassar, R., Golde, T., 2010. The secretases: enzymes with therapeutic potential in Alzheimer disease. Nat. Rev. Neurol. 6, 99–107.

Deacon, R.M.J., 2006. Assessing nest building in mice. Nat. Protoc. 1, 1117–1119.

Deacon, R.M.J., Cholerton, L.L., Talbot, K., Nair-Roberts, R.G., Sanderson, D.J., Romberg, C., Koros, E., Bornemann, K.D., Rawlins, J.N.P., 2008. Age-dependent and -independent behavioral deficits in Tg2576 mice. Behav. Brain Res. 189, 126–138.

Dennissen, F.J.A., Kholod, N., van Leeuwen, F.W., 2012. The ubiquitin proteasome system in neurodegenerative diseases: culprit, accomplice or victim? Prog. Neurobiol. 96, 190–207.

Doody, R.S., Raman, R., Farlow, M., Iwatsubo, T., Vellas, B., Joffe, S., Kieburtz, K., He, F., Sun, X., Thomas, R.G., Aisen, P.S., Alzheimer's Disease Cooperative Study Steering Committee, Siemers, E., Sethuraman, G., Mohs, R., Semagacestat Study Group, 2013. A phase 3 trial of semagacestat for treatment of Alzheimer's disease. N. Engl. J. Med. 369, 341–350.

Edbauer, D., Winkler, E., Regula, J.T., Pesold, B., Steiner, H., Haass, C., 2003. Reconstitution of gamma-secretase activity. Nat. Cell Biol. 5, 486–488.

Fischer, D.F., van Dijk, R., van Tijn, P., Hobo, B., Verhage, M.C., van der Schors, R.C., Li, K.W., van Minnen, J., Hol, E.M., van Leeuwen, F.W., 2009. Long-term proteasome dysfunction in the mouse brain by expression of aberrant ubiquitin. Neurobiol. Aging 30, 847–863.

Fraser, P.E., Levesque, G., Yu, G., Mills, L.R., Thirlwell, J., Frantseva, M., Gandy, S.E., Seeger, M., Carlen, P.L., St George-Hyslop, P., 1998. Presenilin 1 is actively degraded by the 26S proteasome. Neurobiol. Aging 19, S19–S21.

Fukumori, A., Fluhrer, R., Steiner, H., Haass, C., 2010. Three-amino acid spacing of presenilin endoproteolysis suggests a general stepwise cleavage of gamma-secretase-mediated intramembrane proteolysis. J. Neurosci. 30, 7853–7862.

Garcia-Alloza, M., Robbins, E.M., Zhang-Nunes, S.X., Purcell, S.M., Betensky, R.A., Raju, S., Prada, C., Greenberg, S.M., Bacskai, B.J., Frosch, M.P., 2006. Characterization of amyloid deposition in the APPswe/PS1dE9 mouse model of Alzheimer disease. Neurobiol. Dis. 24, 516–524.

Gentier, R.J., van Leeuwen, F.W., 2015. Misframed ubiquitin and impaired protein quality control: an early event in Alzheimer's disease. Front. Mol. Neurosci. 8, 47.

Gentier, R.J.G., Verheijen, B.M., Zamboni, M., Stroeken, M.M.A., Hermes, D.J.H.P., Küsters, B., Steinbusch, H.W.M., Hopkins, D.A., van Leeuwen, F.W., 2015. Localization of mutant ubiquitin in the brain of a transgenic mouse line with proteasomal inhibition and its validation at specific sites in Alzheimer's disease. Front. Neuroanat. 9, 26.

Goedert, M., Spillantini, M.G., 2006. A century of Alzheimer's disease. Science 314, 777–781.

Gouras, G.K., Almeida, C.G., Takahashi, R.H., 2005. Intraneuronal Abeta accumulation and origin of plaques in Alzheimer's disease. Neurobiol. Aging 26, 1235–1244.

Grimm, M.O.W., Haupenthal, V.J., Mett, J., Stahlmann, C.P., Blümel, T., Mylonas, N.T., Endres, K., Grimm, H.S., Hartmann, T., 2016. Oxidized docosahexaenoic acid species and lipid peroxidation products increase amyloidogenic amyloid precursor protein processing. Neurodegener Dis. 16, 44–54.

Grimm, M.O.W., Haupenthal, V.J., Rothhaar, T.L., Zimmer, V.C., Grösgen, S., Hundsdörfer, B., Lehmann, J., Grimm, H.S., Hartmann, T., 2013. Effect of different phospholipids on α-secretase activity in the non-amyloidogenic pathway of Alzheimer's disease. Int. J. Mol. Sci. 14, 5879–5898.

Gundersen, H.J., Jensen, E.B., 1987. The efficiency of systematic sampling in stereology and its prediction. J. Microsc. 147, 229–263.

Hardy, J., De Strooper, B., 2017. Alzheimer's disease: where next for anti-amyloid therapies? Brain 140, 853–855.

Hardy, J., Selkoe, D.J., 2002. The amyloid hypothesis of Alzheimer's disease: progress and problems on the road to therapeutics. Science 297, 353–356.

Hong, L., Huang, H.-C., Jiang, Z.-F., 2014. Relationship between amyloid-beta and the ubiquitin-proteasome system in Alzheimer's disease. Neurol. Res. 36, 276–282.

Hong, S., Beja-Glasser, V.F., Nfonoyim, B.M., Frouin, A., Li, S., Ramakrishnan, S., Merry, K.M., Shi, Q., Rosenthal, A., Barres, B.A., Lemere, C.A., Selkoe, D.J., Stevens, B., 2016. Complement and microglia mediate early synapse loss in Alzheimer mouse models. Science 352, 712–716.

Hope, A.D., de Silva, R., Fischer, D.F., Hol, E.M., van Leeuwen, F.W., Lees, A.J., 2003. Alzheimer's associated variant ubiquitin causes inhibition of the 26S proteasome and chaperone expression. J. Neurochem. 86, 394–404.

International Genomics of Alzheimer's Disease Consortium (IGAP), 2015. Convergent genetic and expression data implicate immunity in Alzheimer's disease. Alzheimers Dement. 11, 658–671.

Irmler, M., Gentier, R.J.G., Dennissen, F.J.A., Schulz, H., Bolle, I., Hölter, S.M., Kallnik, M., Cheng, J.J., Klingenspor, M., Rozman, J., Ehrhardt, N., Hermes, D.J.H.P., Gailus-Durner, V., Fuchs, H., Hrabě de Angelis, M., Meyer, H.E., Hopkins, D.A., van Leeuwen, F.W., Beckers, J., 2012. Long-term proteasomal inhibition in transgenic mice by UBB^{+1} expression results in dysfunction of central respiration control reminiscent of brainstem neuropathology in Alzheimer patients. Acta Neuropathol. 124, 187–197.

Jankowsky, J.L., Fadale, D.J., Anderson, J., Xu, G.M., Gonzales, V., Jenkins, N.A., Copeland, N.G., Lee, M.K., Younkin, L.H., Wagner, S.L., Younkin, S.G., Borchelt, D.R., 2004. Mutant presenilins specifically elevate the levels of the 42 residue beta-amyloid peptide in vivo: evidence for augmentation of a 42-specific gamma secretase. Hum. Mol. Genet. 13, 159–170.

Jankowsky, J.L., Slunt, H.H., Ratovitski, T., Jenkins, N.A., Copeland, N.G., Borchelt, D.R., 2001. Co-expression of multiple transgenes in mouse CNS: a comparison of strategies. Biomol. Eng. 17, 157–165.

Janus, C., Flores, A.Y., Xu, G., Borchelt, D.R., 2015. Behavioral abnormalities in APPSwe/PS1dE9 mouse model of AD-like pathology: comparative analysis across multiple behavioral domains. Neurobiol. Aging 36, 2519–2532.

Jurisch-Yaksi, N., Sannerud, R., Annaert, W., 2013. A fast growing spectrum of biological functions of γ-secretase in development and disease. Biochim. Biophys. Acta 1828, 2815–2827.

Keller, J.N., Hanni, K.B., Markesbery, W.R., 2001. Impaired proteasome function in Alzheimer's disease. J. Neurochem. 75, 436–439.

Kopan, R., Ilagan, M.X.G., 2004. Opinion: γ-Secretase: proteasome of the membrane? Nat. Rev. Mol. Cell Biol. 5, 499–504.

Krutauz, D., Reis, N., Nakasone, M.A., Siman, P., Zhang, D., Kirkpatrick, D.S., Gygi, S.P., Brik, A., Fushman, D., Glickman, M.H., 2014. Extended ubiquitin species are protein-based DUB inhibitors. Nat. Chem. Biol. 10, 664–670.

Lin, Y.-T., Seo, J., Gao, F., Feldman, H.M., Wen, H.-L., Penney, J., Cam, H.P., Gjoneska, E., Raja, W.K., Cheng, J., Rueda, R., Kritskiy, O., Abdurrob, F., Peng, Z., Milo, B., Yu, C.J., Elmsaouri, S., Dey, D., Ko, T., Yankner, B.A., Tsai, L.-H., 2018. APOE4 causes widespread molecular and cellular alterations associated with Alzheimer's disease phenotypes in human iPSC-derived brain cell types. Neuron 98, 1294.

López Salon, M., Morelli, L., Castaño, E.M., Soto, E.F., Pasquini, J.M., 2000. Defective ubiquitination of cerebral proteins in Alzheimer's disease. J. Neurosci. Res. 62, 302–310.

Manavalan, A., Mishra, M., Feng, L., Sze, S.K., Akatsu, H., Heese, K., 2013. Brain site-specific proteome changes in aging-related dementia. Exp. Mol. Med. 45, e39.

Minkeviciene, R., Rheims, S., Dobszay, M.B., Zilberter, M., Hartikainen, J., Fülöp, L., Penke, B., Zilberter, Y., Harkany, T., Pitkänen, A., Tanila, H., 2009. Amyloid beta-induced neuronal hyperexcitability triggers progressive epilepsy. J. Neurosci. 29, 3453–3462.

Müller, U.C., Deller, T., Korte, M., 2017. Not just amyloid: physiological functions of the amyloid precursor protein family. Nat. Rev. Neurosci. 18, 281–298.

Nixon, R.A., 2017. Amyloid precursor protein and endosomal-lysosomal dysfunction in Alzheimer's disease: inseparable partners in a multifactorial disease. FASEB J. 31, 2729–2743.

Ohtake, F., Saeki, Y., Ishido, S., Kanno, J., Tanaka, K., 2016. The K48-K63 branched ubiquitin chain regulates NF-κB signaling. Mol. Cell 64, 251–266.

Otero, M.G., Fernandez Bessone, I., Hallberg, A.E., Cromberg, L.E., De Rossi, M.C., Saez, T.M., Levi, V., Almenar-Queralt, A., Falzone, T.L., 2018. Proteasome stress leads to APP axonal transport defects by promoting its amyloidogenic processing in lysosomes. J. Cell. Sci. 131, jcs214536.

Palop, J.J., Mucke, L., 2010. Amyloid-beta-induced neuronal dysfunction in Alzheimer's disease: from synapses toward neural networks. Nat. Neurosci. 13, 812–818.

Paxinos, G., Franklin, K.B.J., 2001. The mouse brain in stereotaxic coordinates, 2nd ed. Academic Press, San Diego, CA.

Pensalfini, A., Albay, R., Rasool, S., Wu, J.W., Hatami, A., Arai, H., Margol, L., Milton, S., Poon, W.W., Corrada, M.M., Kawas, C.H., Glabe, C.G., 2014. Intracellular amyloid and the neuronal origin of Alzheimer neuritic plaques. Neurobiol. Dis. 71, 53–61.

Podlisny, M.B., Citron, M., Amarante, P., Sherrington, R., Xia, W., Zhang, J., Diehl, T., Levesque, G., Fraser, P., Haass, C., Koo, E.H., Seubert, P., St George-Hyslop, P., Teplow, D.B., Selkoe, D.J., 1997. Presenilin proteins undergo heterogeneous endoproteolysis between Thr291 and Ala299 and occur as stable N- and C-terminal fragments in normal and Alzheimer brain tissue. Neurobiol. Dis. 3, 325–337.

Sannerud, R., Esselens, C., Ejsmont, P., Mattera, R., Rochin, L., Tharkeshwar, A.K., De Baets, G., De Wever, V., Habets, R., Baert, V., Vermeire, W., Michiels, C., Groot, A.J., Wouters, R., Dillen, K., Vints, K., Baatsen, P., Munck, S., Derua, R., Waelkens, E., Basi, G.S., Mercken, M., Vooijs, M., Bollen, M., Schymkowitz, J., Rousseau, F., Bonifacino, J.S., Van Niel, G., De Strooper, B., Annaert, W., 2016. Restricted location of PSEN2/γ-secretase determines substrate specificity and generates an intracellular Aβ pool. Cell 166, 193–208.

Scheltens, P., Blennow, K., Breteler, M.M.B., De Strooper, B., Frisoni, G.B., Salloway, S., Van der Flier, W.M., 2016. Alzheimer's disease. Lancet 388, 505–517.

Selkoe, D.J., Hardy, J., 2016. The amyloid hypothesis of Alzheimer's disease at 25 years. EMBO Mol. Med. 8, 595–608.

Small, S.A., Simoes-Spassov, S., Mayeux, R., Petsko, G.A., 2017. Endosomal traffic jams represent a pathogenic hub and therapeutic target in Alzheimer's disease. Trends Neurosci. 40, 592–602.

Smith, P.K., Krohn, R.I., Hermanson, G.T., Mallia, A.K., Gartner, F.H., Provenzano, M.D., Fujimoto, E.K., Goeke, N.M., Olson, B.J., Klenk, D.C., 1985. Measurement of protein using bicinchoninic acid. Anal. Biochem. 150, 76–85.

Sosna, J., Philipp, S., Albay, R., Reyes-Ruiz, J.M., Baglietto-Vargas, D., LaFerla, F.M., Glabe, C.G., 2018. Early long-term administration of the CSF1R inhibitor PLX3397 ablates microglia and reduces accumulation of intraneuronal amyloid, neuritic plaque deposition and pre-fibrillar oligomers in 5XFAD mouse model of Alzheimer's disease. Mol. Neurodegener 13, 11.

Steiner, H., Capell, A., Pesold, B., Citron, M., Kloetzel, P.M., Selkoe, D.J., Romig, H., Mendla, K., Haass, C., 1998. Expression of Alzheimer's disease-associated presenilin-1 is controlled by proteolytic degradation and complex formation. J. Biol. Chem. 273, 32322–32331.

Szaruga, M., Munteanu, B., Lismont, S., Veugelen, S., Horré, K., Mercken, M., Saido, T.C., Ryan, N.S., De Vos, T., Savvides, S.N., Gallardo, R., Schymkowitz, J., Rousseau, F., Fox, N.C., Hopf, C., De Strooper, B., Chávez-Gutiérrez, L., 2017. Alzheimer's-causing mutations shift Aβ length by destabilizing γ-secretase-Aβn Interactions. Cell 170, 443–456.e14.

Tan, Z., Sun, X., Hou, F.-S., Oh, H.-W., Hilgenberg, L.G.W., Hol, E.M., van Leeuwen, F.W., Smith, M.A., O'Dowd, D.K., Schreiber, S.S., 2007. Mutant ubiquitin found in Alzheimer's disease causes neuritic beading of mitochondria in association with neuronal degeneration. Cell Death Differ. 14, 1721–1732.

Thinakaran, G., Borchelt, D.R., Lee, M.K., Slunt, H.H., Spitzer, L., Kim, G., Ratovitsky, T., Davenport, F., Nordstedt, C., Seeger, M., Hardy, J., Levey, A.I., Gandy, S.E., Jenkins, N.A., Copeland, N.G., Price, D.L., Sisodia, S.S., 1996. Endoproteolysis of presenilin 1 and accumulation of processed derivatives in vivo. Neuron 17, 181–190.

Tseng, B.P., Green, K.N., Chan, J.L., Blurton-Jones, M., LaFerla, F.M., 2008. Abeta inhibits the proteasome and enhances amyloid and tau accumulation. Neurobiol. Aging 29, 1607–1618.

Tucker, S.M.F., Borchelt, D.R., Troncoso, J.C., 2008. Limited clearance of pre-existing amyloid plaques after intracerebral injection of Abeta antibodies in two mouse models of Alzheimer disease. J. Neuropathol. Exp. Neurol. 67, 30–40.

van Leeuwen, F.W., de Kleijn, D.P.V., van den Hurk, H.H., Neubauer, A., Sonnemans, M.A.F., Sluijs, J.A., Köycü, S., Ramdjielal, R.D.J., Salehi, A., Martens, G.J.M., Grosveld, F.G., Burbach, J.P.H., Hol, E.M., 1998. Frameshift mutants of beta amyloid precursor protein and ubiquitin-B in Alzheimer's and Down patients. Science 279, 242–247.

van Tijn, P., De Vrij, F.M.S., Schuurman, K.G., Dantuma, N.P., Fischer, D.F., van Leeuwen, F.W., Hol, E.M., 2007. Dose-dependent inhibition of proteasome activity by a mutant ubiquitin associated with neurodegenerative disease. J. Cell. Sci. 120, 1615–1623.

van Tijn, P., Dennissen, F.J.A., Gentier, R.J.G., Hobo, B., Hermes, D., Steinbusch, H.W.M., van Leeuwen, F.W., Fischer, D.F., 2012. Mutant ubiquitin decreases amyloid β plaque formation in a transgenic mouse model of Alzheimer's disease. Neurochem. Int. 61, 739–748.

van Tijn, P., Verhage, M.C., Hobo, B., van Leeuwen, F.W., Fischer, D.F., 2010. Low levels of mutant ubiquitin are degraded by the proteasome in vivo. J. Neurosci. Res. 88, 2325–2337.

Venegas, C., Kumar, S., Franklin, B.S., Dierkes, T., Brinkschulte, R., Tejera, D., Vieira-Saecker, A., Schwartz, S., Santarelli, F., Kummer, M.P., Griep, A., Gelpi, E., Beilharz, M., Riedel, D., Golenbock, D.T., Geyer, M., Walter, J., Latz, E., Heneka, M.T., 2017. Microglia-derived ASC specks cross-seed amyloid-β in Alzheimer's disease. Nature 552, 355–361.

Verheijen, B.M., Gentier, R.J.G., Hermes, D.J.H.P., van Leeuwen, F.W., Hopkins, D.A., 2017. Selective transgenic expression of mutant ubiquitin in Purkinje cell stripes in the cerebellum. Cerebellum 16, 746–750.

Volianskis, A., Køstner, R., Mølgaard, M., Hass, S., Jensen, M.S., 2010. Episodic memory deficits are not related to altered glutamatergic synaptic transmission and plasticity in the CA1 hippocampus of the APPswe/PS1δE9-deleted transgenic mice model of ß-amyloidosis. Neurobiol. Aging 31, 1173–1187.

Voytyuk, I., De Strooper, B., Chávez-Gutiérrez, L., 2018. Modulation of γ- and β-secretases as early prevention against Alzheimer's disease. Biol. Psychiatry 83, 320–327.

Wolfe, M.S., Xia, W., Ostaszewski, B.L., Diehl, T.S., Kimberly, W.T., Selkoe, D.J., 1999. Two transmembrane aspartates in presenilin-1 required for presenilin endoproteolysis and gamma-secretase activity. Nature 398, 513–517.

Woodruff, G., Young, J.E., Martinez, F.J., Buen, F., Gore, A., Kinaga, J., Li, Z., Yuan, S.H., Zhang, K., Goldstein, L.S.B., 2013. The presenilin-1 ΔE9 mutation results in reduced γ-secretase activity, but not total loss of PS1 function, in isogenic human stem cells. Cell Rep. 5, 974–985.